Combined electromagnetic and static structural simulation to reduce the weight of a Permanent Magnet machine rotor for HEV application

Benedikt Groschup[1], Franco Leonardi[2]

[1]RWTH Aachen University. (Formerly with Ford Motor Company), Aachen, Germany, benedikt.groschup@rwth-aachen.de
[2]Research and Advanced Engineering. Ford Motor Company, Dearborn, USA, fleonar2@ford.com

Abstract — **This paper describes a method to achieve minimal rotor weight while maintaining nominal torque, torque ripple and mechanical stress. The approach makes use of combined electromagnetic FEA, static structural FEA and a hybrid genetic algorithm. The work shows that only by introducing mechanical features that reduce stress in the outermost portion of the rotor lamination it is possible to improve significantly on the design weight. After the introduction of slits at the rotor outer diameter, an 11.2% rotor weight reduction is achieved by enlarging the cooling channels.**

Keywords— ***Machine optimization, weight reduction, HEVs, IPM***

I. INTRODUCTION

Emission reduction and improvement of fuel consumption are driving factors in the research of automotive powertrains. Ford Motor Company faces these challenges with extensive research in the field of electrified vehicles. The electric machine is a central component in electrified powertrains and thus a significant part in achieving development targets. Electric machine studies have historically focused on performance or cost reduction, while mechanical requirements were treated as design refinements and were considered in successive investigations. However, as electromagnetic designs become more and more refined, the focus is shifting to secondary targets, like weight reduction and noise vibration and harshness (NVH), where gains are measured in grams and decibels. Geometrical adjustments, performed to ensure a design within the mechanical load limits, affect the electromagnetic performance and NVH behavior, and this cross coupling requires an iterative optimization process until all conditions are properly met. This causes the computational cost of the approach to increase significantly and demands an efficient and highly automated approach to multi objective optimization.

II. TECHNICAL APPROACH TO COMBINED SIMULATION

In the present study, the weight of an electric motor rotor is optimized and the conflicting objectives are addressed by a combined electromagnetic and static structural multi-objective optimization approach (Fig. 1). As the 10 month study conducted at the Ford Research and Innovation Center utilizes commercial software, the contribution of this paper are not found in the code used to obtain the results, but in the engineering of the solutions and the many comments and
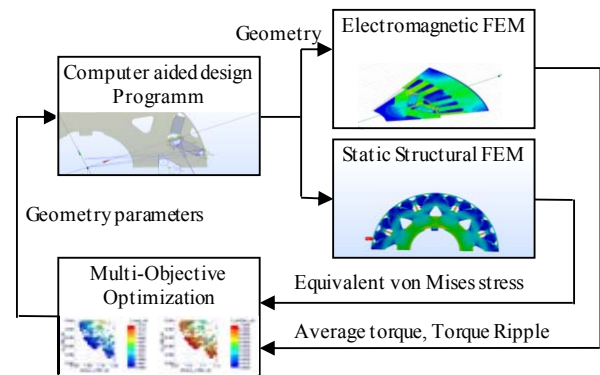

Fig. 1. Flow chart of combined electromagnetic and static structural optimization model

suggestions provided throughout the paper. The geometry is generated in computer-aided design software (Ansys Design Modeler) and then sent to an electromagnetic and a static structural finite element model (Ansys Maxwell and Static Structural package). To monitor electromagnetic performance, the average torque at maximum current is calculated in the electromagnetic simulation. The motor specifications, operation points, and main variables are shown in Table 1.

The weight optimized rotor needs to meet noise requirements. Common methodologies found in literature focus

TABLE 1. MACHINE PARAMETERS

Specification	Variable	Value	Unit
Maximum rotational speed	n	15,500	Rpm
Rotor outer radius	r_o	75.4	Mm
Rotor inner radius	r_i	29.0	Mm
Pole pairs	p	4	
Number of stator slots	x	48	
Maximum stator current	I	500	A
Maximum allowable stress	σ'	207	MPa
Poisson's ratio	ν	0.3	
Density of rotor	ρ	7650	kg/m3

either on torque ripple causing vibrations on driving shaft and transmission, or on radial and tangential forces acting on stator teeth that lead to vibrations in the housing. [2], [4], [5], [7]. The present study uses torque ripple as an indicator of NVH behavior leading to short calculation time as the necessary data is obtained directly from the electromagnetic finite element simulation model. The equivalent von Mises (EVM) stress under centrifugal load is monitored to ensure sufficient rotor durability. The stresses in the electrical steel lamination with steel grade JFE 35JNE250 are calculated using 2D plane stress as the most conservative method for calculation [6], [1].

$$\sigma' = \sqrt{\sigma_x^2 - \sigma_x \sigma_y + \sigma_y^2 + 3\tau_{xy}^2} \qquad (1)$$

Where σ_x and σ_y are the normal stresses in x- and y-direction and $\tau_{x,y}$ is the shear stress. Additional loads, due to thermal expansion, axial clamp forces, and electromagnetic forces, are determined to have minor influence in this application [3]. Several challenges that are beyond the scope of this paper needed to be addressed in the development process of the coupled simulation methodology. Whereas for electromagnetic simulation a coarse geometry is acceptable, for static structural simulation a smooth geometry is necessary. Therefore all features in the CAD program were implemented with tangential transition. An automatic mesh refinement methodology for the static structural FEM simulation was implemented. A description and comparison of state of the art mesh refinement methodologies can be found in [8], [9], [10]. A comprehensive mesh refinement study requires at least three refined meshes to calculate relative absolute error and convergence rate. In this paper, an alternative methodology with only two steps to judge convergence is used and convergence rate is not calculated. The two step approach is available in Ansys static structural environment, but leads to higher risk of misjudging convergence in case of a weak singularity with small but decreasing stress increments. A relative absolute error of 1% and a mesh refinement factor of 2 is used for excellent level of convergence. For the present study, manual three step mesh refinement were compared to automatic two step mesh refinement for static structural FEM with a maximum deviation in the EVM stress of 0.6%. Undesired influences of singularities that caused local areas of high stress had to be removed from consideration for the optimization process to yield meaningful results. [8], [9], [10]

The multi-objective optimization approach was implemented in ModeFrontier to drive the coupled electromagnetic and static structural simulation. 19 input variables were manipulated by means of a hybrid algorithm which combines the global exploration capabilities of Genetic Algorithms with the accurate local exploitation guaranteed by Sequential Quadratic Programming implementations. The input parameters are geometric dimensions of the oil hole as discussed in section V and of the other features introduced to release stress from the lamination. The magnet pocket is intentionally left out of the optimization. Of the 17 output variables, two are defined as objective function to be minimized (weight and maximum overall lamination EVM stress), two (output torque and torque ripple) are used as constrains not to be exceeded and the rest (EVM stress value in specific areas of the lamination) are used

for information and monitoring purposes. Chain dimensioning is intentionally used to avoid intersecting geometries leading to high number of invalid simulation runs (see section V).

III. HOLDING BANDS

The primary hurdle to weight reduction is the rapid increase of the lamination stress as soon as the lamination is modified to increase the size of the various cut outs. To address this issue, the present paper focuses on improving the stress distribution in the rotor caused by centrifugal load. First, the influence of tangential and radial stress on EVM stress is studied based on a simplified geometry. The results are then transferred to the complex rotor geometry in order to identify limiting areas for weight reduction and proper variables for the optimization.

For the simplified study of the dependencies for EVM stress criteria, a thin rotating ring with constant thickness under 2D plane stress is studied. The normal stresses in tangential σ_t and radial σ_r direction can be calculated as [11]

$$\sigma_t = 4\rho\pi^2 n^2 \left(\frac{3+\nu}{8}\right) \left(r_i^2 + r_o^2 + \frac{r_i^2 r_o^2}{r^2} - \frac{1+3\nu}{3+\nu} r^2\right) \qquad (2)$$

$$\sigma_r = 4\rho\pi^2 n^2 \left(\frac{3+\nu}{8}\right) \left(r_i^2 + r_o^2 - \frac{r_i^2 r_o^2}{r^2} - r^2\right) \qquad (3)$$

The values for the density ρ, the poisson's ratio ν, and the rotational speed n are shown in Table 1. Neglecting the shear stresses, the EVM stress can be calculated as [6]

$$\sigma' = \sqrt{\sigma_r^2 - \sigma_r \sigma_t + \sigma_t^2} \qquad (4)$$

The tangential, radial, and EVM stress as a function of the radius r for the simplified geometry is shown in Fig. 2. The comparison identifies tangential stress as the dominant influence factor on EVM stress. The radial component has a minor impact. In other words, the centrifugal load is sustained by areas in the lamination that are able to carry tangential stress i.e. the areas are not cut by the magnet pockets or the cooling channels in the
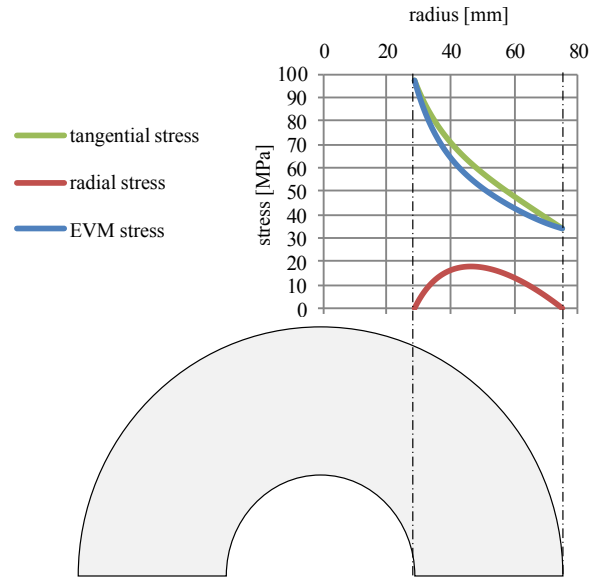

Fig. 2. Stress distribution for a thin hollow cylinder under centrifugal load

geometry. Three areas without cut outs in tangential direction are identified in the baseline design and are referred to as holding bands from this point forward (see Fig. 5). The maximum EVM stress on the lamination occurs at geometry features next to these areas (see Fig. 5 left). The stress in these features (i.e. the top-side-bridge and the key-cut-out) are the primary factors that limit significant weight reduction.

A good understanding of the cross coupling between the holding bands is necessary for the selection of an effective optimization strategy. Equation (2) – (4) show the influence of inner and outer radius on the global maximum EVM stress in the simplified lamination e.g. a change of the laminations inner diameter leads to changed EVM stress on the entire lamination. This cross coupling can also be monitored in the complex rotor lamination using numerical evaluation of a 1/16 static structural model (see Fig. 3). The inner radius is varied in steps of 0.5mm from 27mm to 31mm. An increased inner radius leads to decreased width of the inner holding band. This leads to a higher stress distribution in all holding bands and finally to increased EVM stress on the top-side-bridge and the cooling-channel. The centrifugal forces of the magnets and the outer portion of the lamination i.e. the portion beyond the bridges, has to be sustained by both the top-side-bridges and the center-bridge. Therefore, the maximum EVM stress on the center-bridge slightly decreases with increasing top-side-bridge stress. (see Fig. 3)
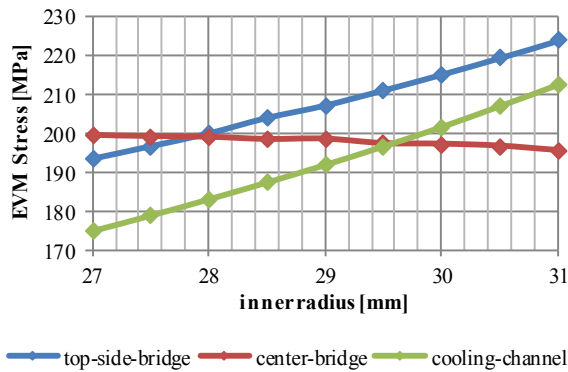
IV. STRESS REDUCTION

In the baseline design, the EVM stress on the top-side-bridge is the limiting factor for weight reduction due to the dependency between stresses in the inner and outer holding band. Thus, a reduction of top-side-bridge stress is key to enable further weight reduction. One commonly discussed design factor is the bridge thickness. Increased thickness leads to decreased EVM stress in the bridges. However, this also leads to increased magnetic flux leakage and penalties in electromagnetic design [3]. This paper presents an alternative approach for stress reduction i.e. Outer-Diameter-Cut-Outs (ODCOs). This feature aims to cuts through the holding band located at the outer diameter (see Fig. 4) and reduces tangential stress in the bridges. Thereby the EVM stress distribution on the top-side-bridges is reduced and potential for additional weight reduction is created. The feature is designed with three parameters i.e. the width (W_01), the length (L_01) and the radius of the end cavity (R_01).

In a first study the influence of the feature on the EVM stress distribution of the center-bridge and the top-side-bridges is determined. A 1/16 static structural model is used. The width of the feature is kept constant to 0.4 mm and the radius is kept to 0.4mm. L_01 is varied between 0 mm and 15mm in steps of 1.5mm. The EVM stress of the center-bridge and the top-side bridge are calculated. Thereby, the top-side-bridge is divided into an inner and an outer portion (see Fig. 6). The results of the calculation are shown in Fig. 7. The stress on the inner portion
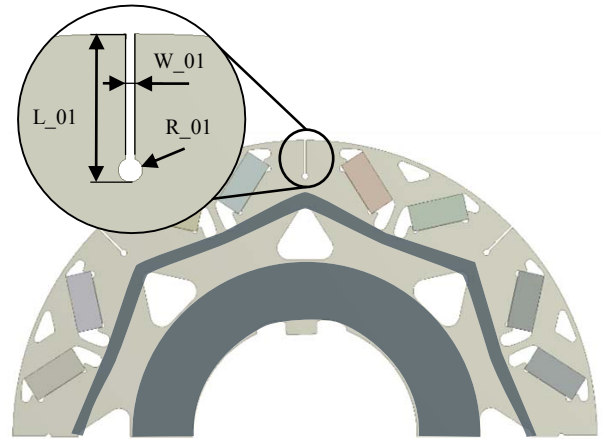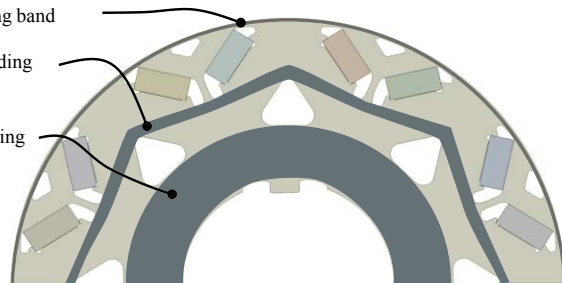

Fig. 3. Influence of inner radius on EVM stress distribution

Fig. 4 : Holding bands of lamination with ODCOs in a 1/2 static structural rotor model

Fig. 5. Holding bands in rotor lamination in 1/2 static structural rotor model

- ▪▪▪ center-bridge
- ▪▪▪ top-side-bridge inner portion
- ▪▪▪ top-side-bridge outer portion
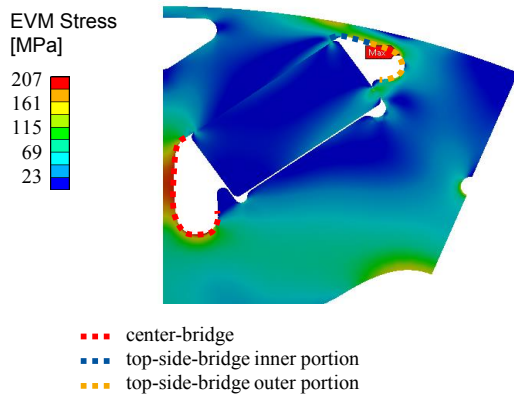
Fig. 6. Selection of stress areas for stress reduction study in 1/16 static structural model

- center-bridge
- top-side-bridge: inner portion
- top-side-bridge: outer portion

Fig. 7. Influence of Length of ODCOs on EVM stress in center-bridge and top-side bridge

of the top-side-bridge decreases with an increased length of the feature, while the stress on the outer portion increases for a length up to 7.5mm and decreases afterwards. This effect can be explained by the stress path between two neighboring bridges. On the one hand the strength of the outer holding band is decreased leading to lower stress in the top-side bridge. On the other hand, the stress path of the feature is pushed towards the outer portion of the top-side-bridge and thus bypassed by the rounding of the outer portion of the top-side-bridge which leads to increased stress in this portion. The superposition of these two effects leads to the behavior in the stress plot. The centrifugal load of the portion of the lamination beyond the bridges as well as the magnets has to be sustained by both the top-side-bridge and the center-bridge. Therefore, the stress on the center bridge increases as the outer holding band is weakened.

The stress reduction study proves the capability of the ODCOs to reduce the stress in the top side bridge. The length of the feature needs to be included in the weight optimization study as the point of intersection between the stresses on the outer and the inner portion of the top-side-bridge stress is influenced by the size of the cooling-channel.

V. WEIGHT REDUCTION

In the present paper, the influence of the key-cut-out is neglected in order to reduce the model size from half the rotor to 1/16th of it. The details of the curvature of the lamination near the key-cut-out is responsible for high stress located at this feature and can easily be optimized in a successive step in case maximum EVM stress occurs there.

The weight reduction study aims to enlarge the transmission fluid cooling channel in the rotor q-axis or add additional holes in the lamination. Three different approaches of cooling channel optimization are performed based on a 1/16 static structural rotor model to ensure high computational performance (see Fig. 8). The three approaches are both calculated with and without ODCOs resulting in a total of six optimizations. For the ODCOs same settings for the variables are used like shown in section IV, i.e. one variable (L_01) is manipulated. All three approaches
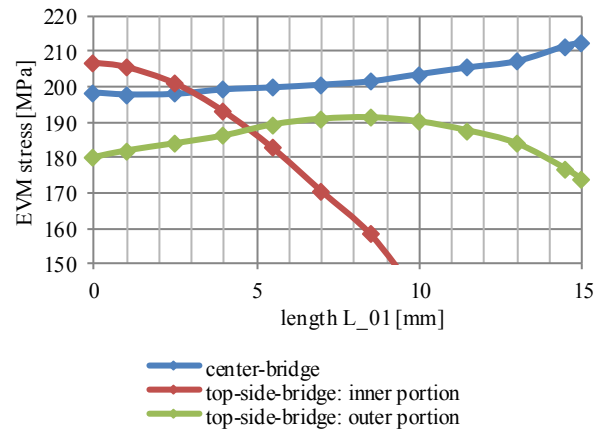
aim to keep previously described holding bands as well as necessary flux path for reluctance torque constant and add holes where material in the sheet is not needed. Encroaching into the flux path causes penalties in torque performance. A reduction of the inner holding band leads to increased stress in the outer holding band and thus to penalties in stress distribution of the bridges. The definition of the manipulated parameters is shown in Fig. 9. The first approach is consistent with the baseline design. The cooling channel is designed with a fully parameterized spline, defined by 10 independent dimensions (see Fig. 9a). Nine variables (L_02 - L_10) are used to define the size and the shape of the spline and an additional variable (R_02) defines the radial position of the cooling-channel. The channel is driven to fit into the space between the holding bands and the flux path. In the second approach, an additional cavity in the rotor's d-axis is introduced. The cavity is designed with a combination of two lines and an oval shape that joins the lines (see Fig. 9b). For this cavity, one parameter (R_03) is used to define the radial position on the d-axis of the rotor. The transition points between the oval shape and the lines are defined with the width (W_02), the heights (H_01), and two dimensionless factors (F_01 and F_02). The cavity is located in an area that is not used by either the inner holding band or the flux path. The same parameterization of the cooling channel is used. In the third approach (see Fig. 9c), the cooling channel is split in two smaller sections. This has the effect of creating a strong middle holding band that releases tension from the inner holding band. The inner radius (R_04) and the thickness (H_02) of the additional holding bridge provide two additional
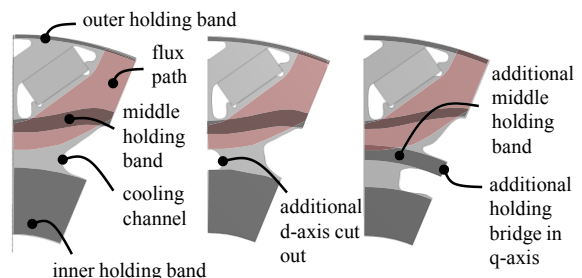

Fig. 8. Three different approaches for weight reduction

a) cooling-channel   b) additional d-axis cut out   c) additional holding bridge
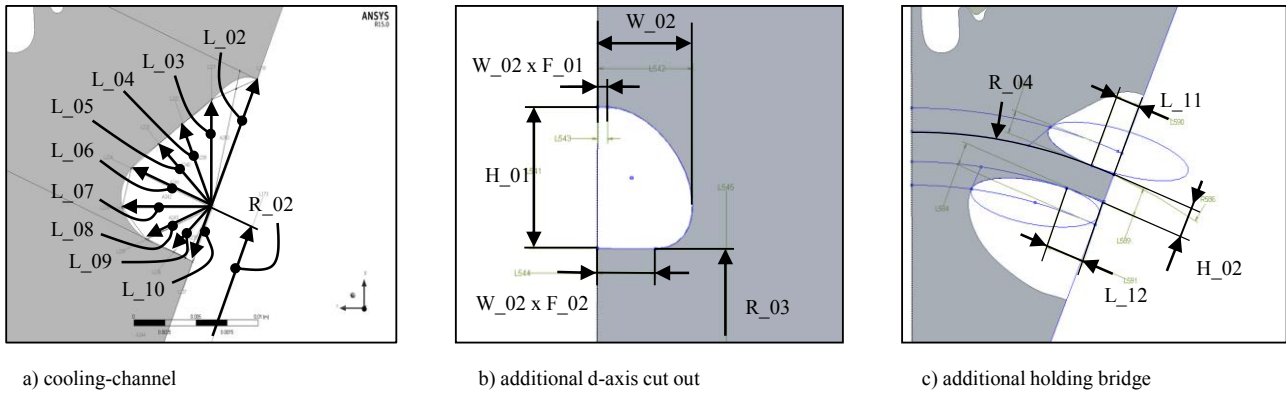
Fig. 9. Geometrical dimensions manipulated by optimization software to achieve weight reduction for the three approaches

optimization parameters. The transition to the cooling channel is realized by two oval shapes with tangential transition (L_11 and L_12).

The mass of the lamination and the peak EVM stress of the lamination are driven to a minimum by the optimization software using the objective goal function. For all runs, the average torque and the torque ripple are restricted to a maximum degradation of 0.5 % using the constraint goal function. An additional constraint for maximum EVM stress is implemented to avoid design points with greater stress values than 120 % of the baseline and improve the efficiency of the optimization. The results are normalized based on the baseline values. The design points on the Pareto front that create a hull curve are extracted for each optimization. As an example for this process, the results of the Pareto optimization for the cooling channel are shown in Fig. 10. Design points that meet all constraints and have the lowest values for rotor weight and stress create the Pareto front and are highlighted in the plot. A comparison of all weight reduction approaches is shown in Fig. 11. The three runs that include the stress relieving ODCO show significantly lower values for the lamination weight. The three best designs that do not show an increase in the overall lamination stress level are selected for a detailed study (see Fig. 12). The average torque at maximum current is constant for all three design-proposals and

shows a maximum degradation of 0.4% compared to baseline. The torque ripple at maximum current varies in a range of 0.7% which is not significant compared to the model's accuracy. The maximum increase in the torque ripple is 0.5% compared to baseline. All three final designs show a mass reduction rate between 10.7% and 11.2% relative to the baseline design. The relative moment of inertia of the lamination about the origin was reduced between 6% and 6.7%. Under restriction of a maximum 115% baseline stress, the three approaches predict a weight reduction between 12.3% and 15.5%).

For all three designs shown in Fig. 12, the cooling-channel was moved slightly toward the shaft. The influence of the changed cooling geometry on the cooling performance of the rotor needs to be studied in following investigations. Further studies need to be done using a 1/2 static structural model with consideration of the key-cut-out. Furthermore, torque ripple was used as an indicator for NVH performance: it is not a direct measurement of it. A comprehensive NVH study needs to be performed considering tooth forces, vibration velocity of the stator and an acoustic simulation model.

VI. CONCLUSION

The presented combined electromagnetic and static structural simulation model is able to identify the best trade-off
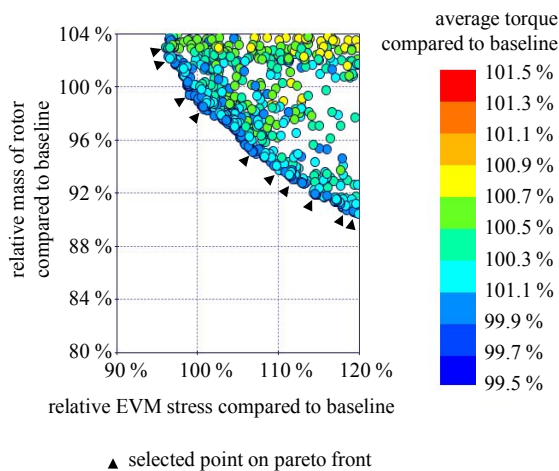

Fig. 10. Results of Pareto optimization for cooling channel and selection of points on Pareto front for comparison
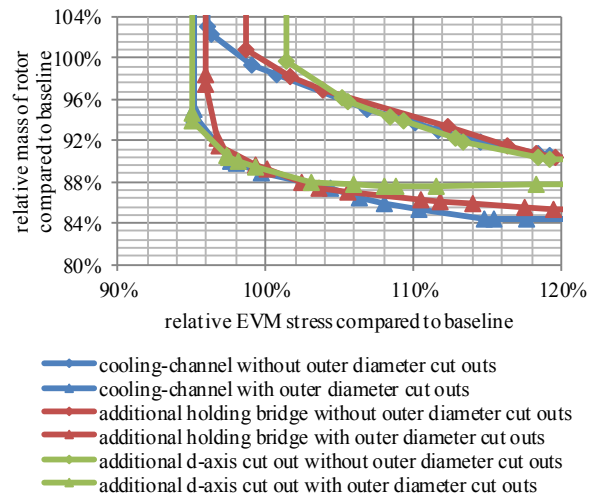

- cooling-channel without outer diameter cut outs
- cooling-channel with outer diameter cut outs
- additional holding bridge without outer diameter cut outs
- additional holding bridge with outer diameter cut outs
- additional d-axis cut out without outer diameter cut outs
- additional d-axis cut out with outer diameter cut outs

Fig. 11. Relative mass and relative EVM stress compared to baseline design

Fig. 12. Detailed results of 100 % overall stress points for approaches with outer diameter cut outs using 1/16 static structural rotor model
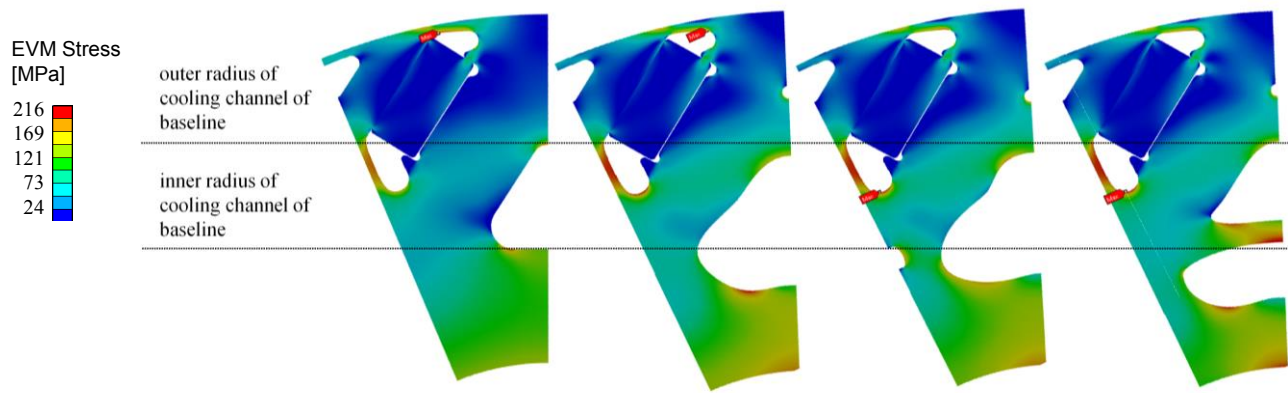
Variable	Baseline	Cooling channel with outer diameter cut out	Additional d-axis cut out with outer diameter cut out	Additional holding bridge in q-axis with outer diameter cut out
Torque ripple at maximum current	100.0 %	100.5 %	100.3 %	99.8 %
Average torque at maximum current	100.0 %	99.6 %	99.6 %	99.6 %
Mass of rotor	100.0 %	88.8 %	89.0 %	89.3 %
Moment of inertia of rotor	100.0 %	93.3%	93.3 %	94.0 %
Equivalent von Mises stress	100.0 %	99.7%	100.3 %	100.1 %

between electromagnetic, mechanical and torque ripple requirements. While torque ripple, average torque at maximum current, and EVM stress are kept constant, the weight of the rotor is reduced by 11.2%. The improvements correspond to a significant weight reduction of 0.97kg and a moment of inertia reduction of $1.8gm^2$ for the rotor of the electric drive, if all boundary conditions are kept constant. The study was exclusively based on the electric motor of the power split hybrid. Assuming a similar weight reduction rate of 11.2% for the generator this would lead to a total weight reduction of 1.45kg. The weight reduction rates show more significant differences in cases where a higher baseline stress is permitted. (see Fig. 11). Key factor for a significant weight reduction in the present study is the optimization of stress distribution between the holding bands in the rotor. The outer-diameter-cut-outs cut through the outer holding band and leads to a stress reduction in the top-side-bridges. This enables an increase in size of the cooling channels, and consequent lamination weight reduction, because the strength of the inner holding band can be reduced without leading to excessive stress in the outer holding band. This weight reduction is a significant contribution to reduce the driving resistances, which leads to improved emission and fuel consumption of the vehicle.

REFERENCES

[1] S. M. Cho, J.K. Kim, H.K. Jung, and C. G. Lee, "Stress and thermal analysis coupled with field analysis of multilayer buried magnet synchronous machine with a wide speed range", IEEE Transactions on Magnetics, vol. 41, no. 5, pp. 1632–1635, May 2005

[2] J. B. Dupont, R. Aydoun, and P. Bouvet, "Simulation of the noise radiated by an automotive electric motor: Influence of the motor defects", SAE International Journal of Alternative Powertrains, vol. 3, no. 2: pp. 310–320, June 2014

[3] Y. Gao, R. Long, Y. Pang, and M. Lindenmo, "Fatigue properties of an electric steel and design of EV/HEV IPM motor rotors for durability and efficiency", SAE Technical Paper 2010-01-1308, April 2010

[4] K. Hameyer and F. Henrotte, "Computation of electromagnetic force densities: Maxwell stress tensor vs. virtual work principle", Journal of Computational and Applied Mathematics, vol 168, no 1-2, pp 235–243, July 2004

[5] P. Pellerey, V. Lanfranchi, and G. Friedrich, "Coupled numerical simulation between electromagnetic and structural models. Influence of the supply harmonics for synchronous machine vibrations", IEEE Transactions on Magnetics, vol. 48, no. 2, pp.983–986, February 2012

[6] B. Riemer, M. Leßemann, and K. Hameyer, "Rotor design of a high speed permanent magnet synchronous machine rating 100,000rpm at 10kW", IEEE Energy Conversion Congress and Exposition (ECCE), pp. 3978–3985, Septermber 2010

[7] M. Senousy, P. Larsen, and P Ding, "Electromagnetics, structural harmonics and acoustics coupled simulation on the stator of an electric motor", International Journal of Passenger Cars- Mechanical Systems, Detroit, vol. 48, no 2, pp. 822–828, SAE, 2014

[8] J. Pointer "Understanding accuracy and discretization error in an FEA model", Pittsburg, International ANSYS Conference, 2004

[9] G. Sinclair, J. Beisheim, and S.Sezer ,, Practical convergence-divergence checks for stresses from FEA", Pittsburg, International Ansys Conference, 2006

[10] G. Sinclair and J.Beisheim "Alternative convergence divergence checks for stresses from FEA", Pittsburg, International Ansys Conference, 2008

[11] R.G. Budynas, J.K. Nisbett, and J. E. Shigley "Shingley's mechanical engineering design" Singapore, McGraw Hill Education, no 8 in si units, 2008